

Molecular Weight Determination of Kuhn Monomers from a Dynamic Property of Polymers

Hiroki Degaki, Loren Jørgensen, Tsuyoshi Koga, and Tetsuharu Narita*



Cite This: *Macromolecules* 2025, 58, 314–320



Read Online

ACCESS |



Metrics & More

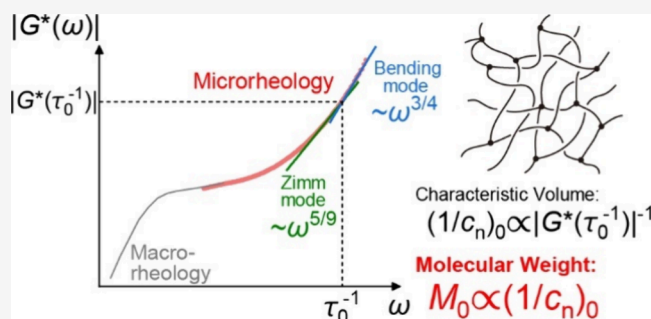


Article Recommendations



Supporting Information

ABSTRACT: Dynamic rheological responses of polymer solutions exhibit a range of dynamic modes reflecting the hierarchical structures with different characteristic lengths such as the Kuhn length and mesh size. The polymer contribution to the viscoelastic modulus at each dynamic mode is proportional to the number density of unit segments at the corresponding hierarchical level, allowing for the determination of their molecular weight. This paper evaluates the molecular weight of a Kuhn monomer from the boundary between the Zimm and bending modes, using a worm like micellar solution of cetylpyridinium chloride/sodium salicylate as a model system. Employing high-frequency diffusing-wave spectroscopy microrheology, we determined the molecular weight, which agrees well with that measured by static light scattering. We showed that the radius of the Kuhn monomer was also accurately estimated from the characteristic volume related with the molecular weight. The proposed method holds potential for application across various dynamic modes and polymer solutions.



INTRODUCTION

Polymer chains in solution and gels exhibit hierarchical structures determined by their chemical compositions and interactions. Static measurements provide insights into these structures and interactions, while dynamic properties, particularly rheological properties, reveal distinct dynamic modes that correspond to various characteristic lengths and interactions within the polymer chain. These dynamic modes allow us to characterize polymer structures in greater detail.^{1,2} Key parameters for describing polymer dynamics include the characteristic lengths of the unit segments, which ranges from small statistical monomer units to the entire chains, and the number of the unit segments, which corresponds to the molecular weight (MW). In dilute polymer solutions, the MW of the entire chain can be determined through zero-shear viscosity measurements.^{1,2} For cross-linked or entangled polymer systems, the MW of the strand can be commonly estimated from the elastic plateau modulus observed at low frequencies.^{3,4} However, to investigate smaller characteristic units, such as Kuhn monomers and correlation blobs, rheological measurements at high frequencies are required.

Microrheology is a practical technique for high-frequency rheometry. It is a relatively new technique developed over the past three decades, which estimates viscoelastic properties by tracking the motion of thermally fluctuating Brownian particles added to a sample.^{5–22} Complementarily used with classical macrorheology, which typically covers frequencies up to around 10^2 rad/s,¹⁵ microrheology extends the accessible frequency range up to approximately 10^5 rad/s.^{5–22} It has been

successfully employed to determine the Kuhn length (or persistence length) of semiflexible wormlike micelles and biopolymers,^{16–20} as well as the correlation length of flexible polymers.¹⁴ However, the MW corresponding to these characteristic lengths has not been fully explored.

This study proposes a rheological method for determining the MW of the small unit segments in polymer chains. We use microrheology to successfully determine the MW of Kuhn monomers, providing detailed characterization of the hierarchical structures of polymer systems. A theoretical concept is experimentally confirmed using wormlike micellar solutions, a well-established model polymeric system in microrheology.^{10,19–22}

EXPERIMENTAL SECTION

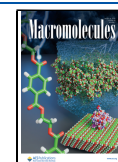
Materials. Cetylpyridinium chloride monohydrate (CPyCl·H₂O) was purchased from TCI, and sodium salicylate (NaSal) from Sigma-Aldrich. An aqueous suspension of polystyrene microspheres (particle size: 500 nm, plain surface) used as probe particles for diffusing-wave spectroscopy (DWS) microrheology experiments was obtained from Micromod (Rostock, Germany). All the chemicals were used as received without further purification.

Received: October 22, 2024

Revised: December 2, 2024

Accepted: December 23, 2024

Published: December 31, 2024



Sample Preparation. CPyCl/NaSal aqueous solutions ([CPyCl]:[NaSal] = 5:3) were prepared by mixing CPyCl·H₂O and NaSal in Milli-Q water at room temperature, then the mixture was heated to 60 °C to ensure homogenization and solubilization of the surfactant. For DWS measurements, the aqueous suspension of the probe particles was added to the CPyCl/NaSal solution at 60 °C. The probe concentration was set to 1 wt %. For SLS measurements, Milli-Q water filtered with a 0.2 μm syringe filter was used. The final CPyCl/NaSal solutions were filtered with a 0.8 μm syringe filter.

Macrorheological Oscillatory Shear Measurements. Oscillatory shear measurements were carried out at 25 °C using a DHR3 stress-controlled rheometer (TA Instruments) with a cone–plate geometry (diameter: 40 mm, angle: 2°) equipped with an antievaporation lid for solutions of 60 mM CPyCl and above, and with Couette concentric cylinders (cup diameter: 30 mm, gap: 1 mm) for 50 mM CPyCl solution. Frequency sweeps were performed with an angular frequency range of 0.01–100 rad/s at 1 to 10% strain in the linear regime, determined beforehand by amplitude sweeps at 1 rad/s.

DWS Microrheology. Measurements were conducted using a laboratory-made setup. A Spectra-Physics Excelsior laser (wavelength: 532 nm, output power: 300 mW) was used as the coherent light source. The laser beam was expanded to about 1 cm in diameter with a beam expander. A plastic cuvette for spectroscopy with a path length $L = 4$ mm was placed in a thermostated sample holder at 25 °C. The scattered light was collected by an optical fiber placed in the transmission geometry, connected to a photon counter. A digital correlator (ALV-7004/USB-FAST, ALV, Lanssen, Germany) was used to treat signals and obtain the intensity autocorrelation function. The theoretical basis of DWS microrheology is given in the [Supporting Information](#).

Static Light Scattering (SLS). SLS measurements were performed with a 3-CGS ALV goniometer system at 25 °C. The molecular weight was determined by the Zimm plot. The details of the Zimm plot are provided in the [Supporting Information](#).

THEORETICAL BASIS

Let us consider a polymer solution where the polymer chains consist of various unit segments with differing lengths, such as Kuhn monomers, correlation blobs, and mesh strands between cross-links. The specific details of these segments will be explained later. Each unit segment contributes to the viscoelasticity of the system, which is described by the stress relaxation modulus $G(t)$ (t denotes time). For many unit segments, $G(t)$ is generally expressed as^{1,2}

$$G(t) \approx \frac{nk_{\text{B}}T}{V} \left(\frac{t}{\tau} \right)^{-\alpha} = c_{\text{n}}k_{\text{B}}T \left(\frac{t}{\tau} \right)^{-\alpha} \quad (1)$$

where n is the number of the unit segments, k_{B} is the Boltzmann constant, T is temperature, V is the system volume, α is the index corresponding to the mode of the segment, $c_{\text{n}} \equiv n/V$ is the number density of the unit segment, and τ is the relaxation time, which is the characteristic time required for the segment to diffuse a distance on the order of its own size. [Equation 1](#) suggests that the stress relaxation modulus arises from the entropic contributions of the unit segments, analogous to the pressure of an ideal gas $p = nk_{\text{B}}T/V$.

At the corresponding relaxation time τ , [eq 1](#) provides the characteristic volume $1/c_{\text{n}}$, in which one unit segment is found. In dynamic viscoelastic analysis, the complex modulus $G^*(\omega)$ (ω denotes frequency) is obtained from $G(t)$ via the Boltzmann superposition principle as $G^*(\omega) = i\omega \int_0^{\infty} G(t) e^{-i\omega t} dt$. This transformation maintains the magnitude of the moduli: $|G^*(\tau^{-1})| \approx G(\tau)$ (theoretical details are provided in the [Supporting Information](#)). Therefore, $1/c_{\text{n}}$ can be directly

determined from the absolute value of the complex modulus at $\omega = \tau^{-1}$:

$$\frac{1}{c_{\text{n}}} \approx \frac{k_{\text{B}}T}{|G^*(\tau^{-1})|} \quad (2)$$

The determined characteristic volume then yields the number-average MW of the unit segment, M , as

$$M = N_{\text{A}}c_{\text{w}} \left(\frac{1}{c_{\text{n}}} \right) \quad (3)$$

where N_{A} is the Avogadro constant, and c_{w} is the polymer weight concentration (mass per unit volume).

As an illustrative example, let us consider the Kuhn monomer (statistical unit segment) of a semiflexible chain. According to classical polymer dynamics, a semiflexible chain exhibits two distinct modes around the Kuhn length b (twice the persistence length).¹ At length scales larger than b , the chain behaves similarly to a flexible chain in dilute solutions, with significant hydrodynamic coupling between solvents and chains, described by the Zimm model and known as the Zimm mode.^{2,3} At length scales smaller than b , the chain exhibits bending modes, behaving like a stiff rod. The relaxation time of the Kuhn monomer, $\tau_0 \equiv \eta_{\text{s}}b^3/k_{\text{B}}T$ (η_{s} is the solvent viscosity), can be determined from the boundary between the Zimm and bending modes, with the corresponding complex moduli described as¹

$$|G^*(\omega)| \approx \begin{cases} c_{\text{n}}k_{\text{B}}T(\tau_0\omega)^{1/3\nu} (\omega < \tau_0^{-1}, \text{ Zimm mode}) \\ c_{\text{n}}k_{\text{B}}T(\tau_0\omega)^{3/4} (\omega > \tau_0^{-1}, \text{ bending mode}) \end{cases} \quad (4)$$

where ν is the Flory exponent, taking values of 0.588 for good solvents and 0.5 for θ solvents. Applying [eqs 2](#) and [3](#) to this case, the characteristic volume of the Kuhn monomer $(1/c_{\text{n}})_0$ and the MW of the Kuhn monomer M_0 are given by

$$\left(\frac{1}{c_{\text{n}}} \right)_0 \approx \frac{k_{\text{B}}T}{|G^*(\tau_0^{-1})|} \quad (5)$$

$$M_0 = N_{\text{A}}c_{\text{w}} \left(\frac{1}{c_{\text{n}}} \right)_0 \quad (6)$$

[Equations 1](#), [2](#), and [3](#) are broadly applicable for determining the characteristic volumes and MWs of various unit segments in polymer chains. A comprehensive theoretical summary for different unit segments found in polymer solutions of semiflexible or flexible chains at varying concentrations is provided in the [Supporting Information](#).

RESULTS AND DISCUSSION

For experimental validation, we used a wormlike micellar solution of cetylpyridinium chloride/sodium salicylate (CPyCl/NaSal) at 25 °C as a model system, representing semidilute solutions of semiflexible chains. This system has been extensively studied in both microrheological and macrorheological studies due to its unique structural and rheological properties, which are relevant to a wide range of applications.^{10,16,19,24–31} The structural and dynamic properties of this wormlike micellar solution are influenced by the surfactant-to-salt concentration ratio, [CPyCl]:[NaSal]. For this study, we prepared solutions with a fixed ratio of [CPyCl]:

[NaSal] = 5:3, chosen for its ease of preparation, stability, and suitability for microrheological experiments due to its rapid dynamics.^{16,19}

Overall Micellar Structure. First, the overall micellar structure was confirmed through macrorheological oscillatory shear measurements. In Figure 1a, the zero-shear viscosity, η_0 ,

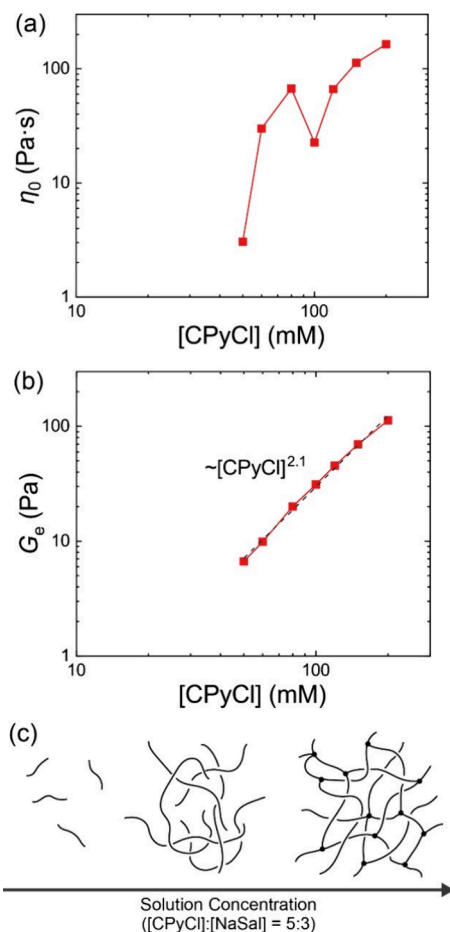


Figure 1. (a, b) Macrorheologically measured (a) zero-shear viscosity η_0 and (b) plateau modulus G_e of the CPyCl/NaSal aqueous solution. The concentration ratio is fixed to [CPyCl]:[NaSal] = 5:3. (c) Estimated structure of wormlike micelles in the investigated CPyCl/NaSal system.

is plotted as a function of the surfactant concentration [CPyCl]. The η_0 value increases with [CPyCl] up to 80 mM, then decreases between 80 and 100 mM, peaking around 80 mM. From 100 mM, η_0 increases again. The peak in the viscosity is characteristic of wormlike micellar solutions undergoing a linear-to-branched transition.^{32–34} Previous studies have reported that η_0 in CPyCl/NaSal solutions reaches a maximum when a linear-to-branched transition occurs as the salt concentration [NaSal] increases at a fixed surfactant concentration [CPyCl].^{16,24} This study observes a similar effect with proportional increases in both [CPyCl] and [NaSal] ([CPyCl]:[NaSal] = 5:3). Surfactants with small head groups and long tail groups such as CPy⁺ generally form linear micelles rather than spherical ones.^{32,35} Initially, as [CPyCl] increases, the linear micelles become longer and more entangled, leading to the increase in η_0 . However, with sufficient salt addition (or increased ionic strength), the electrostatic interactions between cationic charges on the head

groups are screened. This screening makes concave curvature, which brings the charged head groups closer together and reduces the number of end-caps, energetically favorable. Consequently, the wormlike micelles form three- or four-point junctions.³² These branch points can slide along the micellar backbone, relieving stress and leading to the decrease in η_0 .^{32,33} Additionally, temporary branch points (ghost-like crossings) form easily due to reduced energy barriers, contributing to the decrease in η_0 .³² After the decrease, η_0 increases again with further addition of CPyCl due to increased entanglement in the concentrated regime. The rising plateau modulus, G_e , further indicates the increase in entanglements and branching.¹⁶ Within the studied concentration range, G_e increases with [CPyCl] without a noticeable change in trend between 80 and 100 mM, scaling as $G_e \sim [\text{CPyCl}]^{2.1}$ (Figure 1b). The value of the exponent well matches the theoretical prediction (9/4).³⁶ The estimated structure of the wormlike micelles is summarized in Figure 1c.

Microrheology and Conventional Estimation of Kuhn Lengths. Next, we microrheologically measured the complex moduli of these solutions. Diffusing-wave spectroscopy (DWS)⁵ was successfully applied to the CPyCl/NaSal system, consistent with the previous studies.^{10,19,20,22} In Figure 2, we

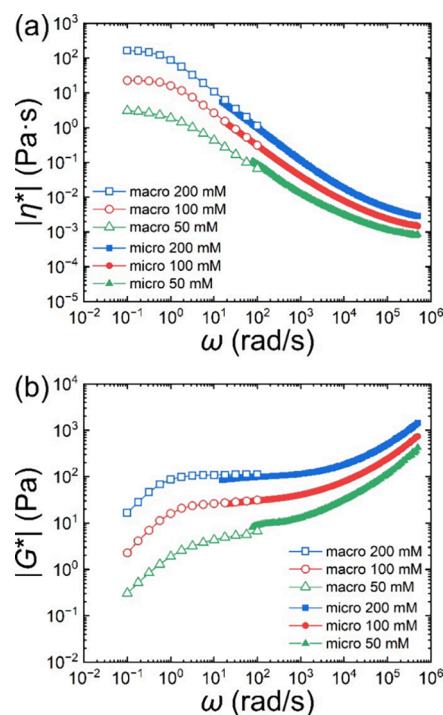


Figure 2. Polymer contribution to (a) complex viscosity and (b) complex moduli of the CPyCl 50, 100, and 200 mM solutions obtained by oscillatory shear macrorheology and DWS micro-rheology.

plotted the complex viscosity and moduli measured by microrheology and macrorheology for three representative CPyCl concentrations (50, 100, and 200 mM). In the overlapping frequency range of about 10–10² rad/s, micro-rheology and macrorheology agree well, with microrheology extending the accessible frequencies up to about 10⁵ rad/s. Figure 3 displays the polymer contribution to the complex modulus from a microrheological measurement for the 100 mM CPyCl solution. We identified the Zimm and bending

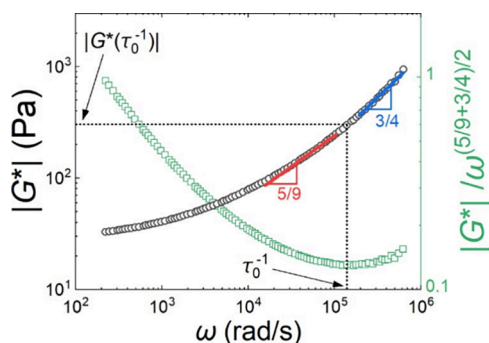


Figure 3. Polymer contribution to complex modulus of the CPyCl 100 mM solution obtained by DWS microrheology (left axis, black circles). The red and blue lines show power-law behaviors with exponents of 5/9 and 3/4, corresponding to the Zimm and bending modes, respectively. Value of $|G^*(\omega)|/\omega^{(5/9+3/4)/2}$ used to determine the crossover point between the two scaling laws (right axis, green squares).

modes, which exhibit power-law behaviors with exponents of 5/9 and 3/4, respectively, as predicted theoretically in eq 4 (note that 5/9 (= 0.56) for the Zimm mode aligns with $1/3\nu$ (= 0.57) for a good solvent where $\nu = 0.588$).^{1,37,38} To determine accurately the crossover point of the two scaling modes, we adopted the method proposed by Tassieri *et al.*, which determines the crossover point from the local minimum of $|G^*(\omega)|/\omega^{(5/9+3/4)/2}$ (the exponent $(5/9 + 3/4)/2$ is the intermediate value between the scaling exponents of each mode).³⁹ The crossover point allows for the determination of the relaxation time τ_0 and the corresponding modulus $|G^*(\tau_0^{-1})|$.

From τ_0 , the Kuhn length can be determined as $b = (k_B T \tau_0 / \eta_s)^{1/3}$. The value of b decreases with increasing surfactant concentration (Figure 4). This behavior, as well as the value of

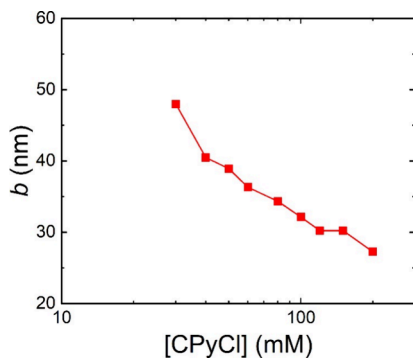


Figure 4. Kuhn length b as a function of [CPyCl].

b , is consistent with the previous studies,^{16,17,40–44} which attribute the decrease to charge screening effects induced by counterions. In our experiments, maintaining a fixed concentration ratio [CPyCl]/[NaSal] means that increasing [CPyCl] also increases the ionic strength. At high ionic strengths, the repulsive forces between the cationic micellar head groups are screened, which enhances chain flexibility. As a result, the length scale at which the chains exhibit bending becomes shorter, leading to the shorter Kuhn length.

Characteristic Volume and Molecular Weight Determination. From $|G^*(\tau_0^{-1})|$, the characteristic volume of the bending mode $(1/c_n)_0$ is determined by using eq 5 and plotted as a function of [CPyCl] in Figure 5 (filled circles). The value

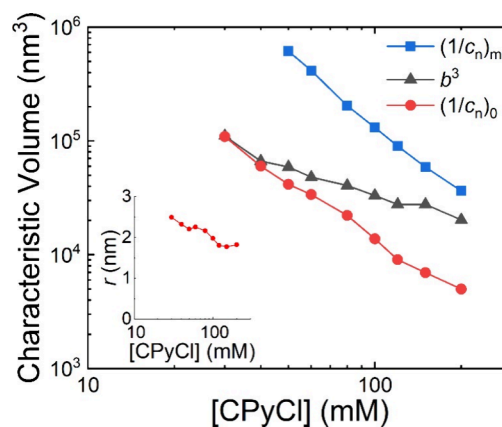


Figure 5. Characteristic volumes as functions of [CPyCl]. The inset shows the radius of the Kuhn monomer calculated from $(1/c_n)_0$.

of $(1/c_n)_0$ decreases with the increase in the concentration, consistent with the decrease in the characteristic length b . We also plotted the value of b^3 in the figure (filled triangles). We found that $(1/c_n)_0 \approx b^3$ at the low concentrations but $(1/c_n)_0 < b^3$ at high concentrations. This result suggests that the distance between neighboring Kuhn monomers is shorter than b . Consequently, the volume $(1/c_n)_0$ that contains both a Kuhn monomer and solvents is space-filling. These volumes repelling each other with interactions on the order of $k_B T$. In other words, each Kuhn monomer and the surrounding solvents form a correlation blob with the volume $(1/c_n)_0$.

In the correlation volume $(1/c_n)_0$ containing one Kuhn monomer and the solvents, the volume fraction of the Kuhn monomer matches that of the entire system, since the correlation volume is space-filling. Thus, the Kuhn monomer volume, v_0 , can be estimated as $v_0 \approx \phi(1/c_n)_0$, where $\phi = c_w/\rho$ is the volume fraction of the surfactant ($\rho \approx 10^3$ g/L is the mass density of the solution). Assuming the Kuhn monomer is cylindrical, we have $v_0 = \pi r^2 b$, where r is the radius of the cylinder. Therefore, the radius can be determined as $r \approx \sqrt{(\phi/\pi b)(1/c_n)_0}$. We found an average radius $r = 2.1 \pm 0.4$ nm over the concentration range of 30–200 mM (the inset in Figure 5), which coincides well with the literature value $r = 2.0 \pm 0.1$ nm, determined by a small-angle neutron scattering.^{45,46} This agreement supports the validity of the microrheological method proposed in this study.

To elucidate the hierarchical structure in this system, the conventional macrorheological method was used to assess the larger characteristic volume. From the elastic plateau modulus G_e , the space-filling volume of the mesh strand (partial chain between the entanglements or branching points) can be determined as⁴

$$\left(\frac{1}{c_n}\right)_m \approx \frac{k_B T}{G_e} \quad (7)$$

Notably, this approach applies eq 2 to a frequency-independent elastic mode ($\alpha = 0$ in eq 1). Although the elastic plateau was also observed in microrheological DWS measurements, macrorheological results (Figure S1b) were preferred over microrheological results (Figure S2) due to their greater accuracy in the low-frequency regime where the plateau appears. The value of $(1/c_n)_m$ plotted in Figure 5 decreases with increasing solution concentration, reflecting greater entanglement and branching. The ratio $(1/c_n)_m/(1/$

$c_n)_0 \approx 7\text{--}14$ suggests that one mesh volume contains approximately 10 Kuhn monomers or correlation blobs.

The MW of the Kuhn monomer M_0 was determined from the value of microrheologically determined $(1/c_n)_0$ or $|G^*(\tau_0^{-1})|$ using eq 6 as shown in Figure 6 (filled circles).

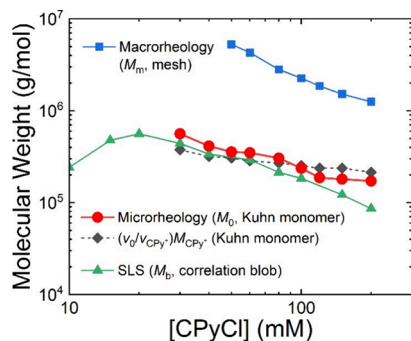


Figure 6. Values of molecular weights (MWs) of three unit-segments determined by different methods as a function of [CPyCl]. MW of the Kuhn monomer M_0 by DWS microrheology (circles), MW of the Kuhn monomer estimated from surfactant monomer MW and volume ratio of the Kuhn monomer to the surfactant monomer (diamonds), MW of the correlation blobs M_b by SLS (triangles), and MW of the mesh strand M_m from plateau modulus measured by oscillatory shear macrorheology (squares).

The value of M_0 decreases with increasing [CPyCl], reflecting the observed reduction in the Kuhn length b . To verify the accuracy of this MW determination method, the determined MW are compared with results obtained from two alternative methods.

The first simple method uses the volume of the Kuhn monomer v_0 and the volume occupied by a single surfactant molecule v_{CPy^+} . A saturated hydrocarbon chain with 16 carbon atoms (cetyl group, CPy^+), has a volume of approximately $v_{\text{CPy}^+} \approx 0.46 \text{ nm}^3$.³⁵ The MW of the Kuhn monomer M_0 is calculated as $M_0 \approx (v_0/v_{\text{CPy}^+})M_{\text{CPy}^+}$, where $M_{\text{CPy}^+} = 287 \text{ g/mol}$ is the MW of CPy^+ , and we have used $r = 2 \text{ nm}$ to calculate $v_0 = \pi r^2 b$. The values of MW are determined and plotted in Figure 6 (filled diamonds). They agree well with those obtained from $|G^*(\tau_0^{-1})|$.

The second method is the static light scattering (SLS) measurement, which provides the MW of the correlation blob M_b through Zimm plots. Scattered light intensity measured by SLS is related to the osmotic pressure Π . It represents the repulsive force between blobs on the order of $k_B T$ as $\Pi \approx c_n k_B T \approx c_w N_A k_B T / M_b$, allowing for the determination of M_b .¹ Figure 6 shows the MW values measured by SLS (filled triangles). In the dilute regime, M_b increases with [CPyCl] due to chain growth, as shown in Figure 1c. At [CPyCl] = 20 mM, it peaks and then decreases with further increases in [CPyCl] due to entanglement and branching of the micelles, which reduces the blob size. Importantly, Figure 6 also shows that M_b from SLS and M_0 from microrheology are in good agreement. This result indicates again that in this system, one correlation blob contains one Kuhn monomer, and M_b and M_0 are equivalent. The proposed microrheological method is as reliable as the conventional SLS measurement.

The MW of the mesh M_m is also evaluated as

$$M_m = N_A c_w \left(\frac{1}{c_n} \right)_m \quad (8)$$

through macrorheological measurements.⁴ Figure 6 demonstrates that M_m decreases with increasing solution concentration, in proportion to $(1/c_n)_m$ (filled squares). Since the mesh occupies a larger volume than the Kuhn monomer and correlation blob, M_m is significantly higher than M_0 and M_b . Note that this previously proposed method is another application of the MW determination method based on eq 3, and that the MW of the different unit segments in the same system can be individually determined from a wide range of modulus.

CONCLUSIONS

We used DWS microrheology to successfully capture the crossover between the Zimm and bending modes in the CPyCl/NaSal wormlike micellar solutions, determining the relaxation time and the corresponding modulus. From these two values, we estimated the Kuhn length, as well as the radius and MW of the Kuhn monomer. The results are consistent with trends observed in the Kuhn length and align with conventional SLS measurements and the estimations based on literature values. Importantly, the MW determination from the modulus at the crossover point of two modes is not specific to either microrheology or wormlike micelles. Theoretically, this method is applicable to a wide range of solutions and gels containing both semiflexible and flexible chains across different concentrations. For example, biopolymers forming ordered rigid structures, such as helices, could be characterized by analyzing their solution dynamics.⁴⁷ Tightly entangled semiflexible polymer solutions could also be studied to provide experimental data for developing theoretical models that describe the relationships among modulus, concentration, and persistence length.^{48,49} Experimental validation in other systems remains a topic for future research.

ASSOCIATED CONTENT

Supporting Information

The Supporting Information is available free of charge at <https://pubs.acs.org/doi/10.1021/acs.macromol.4c02598>.

Theoretical summary for different unit segments, details of DWS microrheology and SLS, supporting figures (PDF)

AUTHOR INFORMATION

Corresponding Author

Tetsuharu Narita – *Laboratoire Sciences et Ingénierie de la Matière Molle, CNRS UMR 7615, ESPCI Paris, Sorbonne Université, PSL Université, Paris 75005, France;*
 orcid.org/0000-0002-2061-1357;
 Email: tetsuharu.narita@espci.fr

Authors

Hiroki Degaki – *Department of Polymer Chemistry, Graduate School of Engineering, Kyoto University, Kyoto 615-8510, Japan;* orcid.org/0009-0006-8897-7669
 Loren Jørgensen – *Laboratoire Sciences et Ingénierie de la Matière Molle, CNRS UMR 7615, ESPCI Paris, Sorbonne Université, PSL Université, Paris 75005, France*
 Tsuyoshi Koga – *Department of Polymer Chemistry, Graduate School of Engineering, Kyoto University, Kyoto 615-8510, Japan;* orcid.org/0009-0003-8366-1719

Complete contact information is available at: <https://pubs.acs.org/10.1021/acs.macromol.4c02598>

Funding

Mazume Research Encouragement Prize in Kyoto University. JSPS KAKENHI Grant Number JP23KJ1326.

Notes

The authors declare no competing financial interest.

ACKNOWLEDGMENTS

The authors thank Théo Merland for fruitful discussions. This work was supported by Mazume Research Encouragement Prize in Kyoto University and JSPS KAKENHI Grant Number JP23KJ1326.

REFERENCES

- (1) Rubinstein, M.; Colby, R. H. *Polymer Physics*; Oxford University Press: New York, 1979.
- (2) Doi, M.; Edwards, S. F. *The Theory of Polymer Dynamics*; Oxford University Press: Oxford, 1986.
- (3) Tuminello, W. H. Molecular Weight and Molecular Weight Distribution from Dynamic Measurements of Polymer Melts. *Polym. Eng. Sci.* **1986**, *26*, 1339–1347.
- (4) Calvet, D.; Wong, J. Y.; Giasson, S. Rheological Monitoring of Polyacrylamide Gelation: Importance of Cross-Link Density and Temperature. *Macromolecules* **2004**, *37*, 7762–7771.
- (5) Mason, T. G.; Weitz, D. A. Optical Measurements of Frequency-Dependent Linear Viscoelastic Moduli of Complex Fluids. *Phys. Rev. Lett.* **1995**, *74*, 1250–1253.
- (6) Mason, T. G.; Ganesan, K.; van Zanten, J. H.; Wirtz, D.; Kuo, S. C. Particle Tracking Microrheology of Complex Fluids. *Phys. Rev. Lett.* **1997**, *79*, 3282–3285.
- (7) Mason, T. G.; Gang, H.; Weitz, D. A. Diffusing-Wave-Spectroscopy Measurements of Viscoelasticity of Complex Fluids. *J. Opt. Soc. Am. A* **1997**, *14*, 139.
- (8) Dasgupta, B. R.; Tee, S.-Y.; Crocker, J. C.; Frisken, B. J.; Weitz, D. A. Microrheology of Polyethylene Oxide Using Diffusing Wave Spectroscopy and Single Scattering. *Phys. Rev. E* **2002**, *65*, No. 051505.
- (9) van Zanten, J. H.; Amin, S.; Abdala, A. A. Brownian Motion of Colloidal Spheres in Aqueous PEO Solutions. *Macromolecules* **2004**, *37*, 3874–3880.
- (10) Buchanan, M.; Atakhorrami, M.; Palierno, J. F.; MacKintosh, F. C.; Schmidt, C. F. High-Frequency Microrheology of Wormlike Micelles. *Phys. Rev. E* **2005**, *72*, No. 011504.
- (11) Squires, T. M.; Mason, T. G. Fluid Mechanics of Microrheology. *Annu. Rev. Fluid Mech.* **2010**, *42*, 413–438.
- (12) Abdala, A. A.; Amin, S.; van Zanten, J. H.; Khan, S. A. Tracer Microrheology Study of a Hydrophobically Modified Comblike Associative Polymer. *Langmuir* **2015**, *31*, 3944–3951.
- (13) Krajina, B. A.; Tropini, C.; Zhu, A.; DiGiuseppe, P.; Sonnenburg, J. L.; Heilshorn, S. C.; Spakowitz, A. J. Dynamic Light Scattering Microrheology Reveals Multiscale Viscoelasticity of Polymer Gels and Precious Biological Materials. *ACS Cent. Sci.* **2017**, *3*, 1294–1303.
- (14) Indei, T.; Narita, T. Microrheological Study of Single Chain Dynamics in Semidilute Entangled Flexible Polymer Solutions: Crossover from Rouse to Zimm Modes. *J. Rheol.* **2022**, *66*, 1165–1179.
- (15) Willenbacher, N.; Oelschlaeger, C. Dynamics and Structure of Complex Fluids from High Frequency Mechanical and Optical Rheometry. *Curr. Opin. Colloid Interface Sci.* **2007**, *12*, 43–49.
- (16) Oelschlaeger, C.; Schopferer, M.; Scheffold, F.; Willenbacher, N. Linear-to-Branched Micelles Transition: A Rheometry and Diffusing Wave Spectroscopy (DWS) Study. *Langmuir* **2009**, *25*, 716–723.
- (17) Galvan-Miyoshi, J.; Delgado, J.; Castillo, R. Diffusing Wave Spectroscopy in Maxwellian Fluids. *Eur. Phys. J. E* **2008**, *26* (4), 369–377.
- (18) Oelschlaeger, C.; Cota Pinto Coelho, M.; Willenbacher, N. Chain Flexibility and Dynamics of Polysaccharide Hyaluronan in Entangled Solutions: A High Frequency Rheology and Diffusing Wave Spectroscopy Study. *Biomacromolecules* **2013**, *14* (10), 3689–3696.
- (19) Willenbacher, N.; Oelschlaeger, C.; Schopferer, M.; Fischer, P.; Cardinaux, F.; Scheffold, F. Broad Bandwidth Optical and Mechanical Rheometry of Wormlike Micelle Solutions. *Phys. Rev. Lett.* **2007**, *99* (6), No. 068302.
- (20) Sarmiento-Gomez, E.; Lopez-Diaz, D.; Castillo, R. Microrheology and Characteristic Lengths in Wormlike Micelles Made of a Zwitterionic Surfactant and SDS in Brine. *J. Phys. Chem. B* **2010**, *114*, 12193–12202.
- (21) Hassan, P. A.; Bhattacharya, K.; Kulshreshtha, S. K.; Raghavan, S. R. Microrheology of Wormlike Micellar Fluids from the Diffusion of Colloidal Probes. *J. Phys. Chem. B* **2005**, *109*, 8744–8748.
- (22) Nishi, K.; Kilfoil, M. L.; Schmidt, C. F.; MacKintosh, F. C. A Symmetrical Method to Obtain Shear Moduli from Microrheology. *Soft Matter* **2018**, *14* (19), 3716–3723.
- (23) Zimm, B. H. Dynamics of Polymer Molecules in Dilute Solution: Viscoelasticity, Flow Birefringence and Dielectric Loss. *J. Chem. Phys.* **1956**, *24*, 269–278.
- (24) Rehage, H.; Hoffmann, H. Rheological Properties of Viscoelastic Surfactant Systems. *J. Phys. Chem.* **1988**, *92*, 4712–4719.
- (25) Berret, J.-F.; Appell, J.; Porte, G. Linear Rheology of Entangled Wormlike Micelles. *Langmuir* **1993**, *9*, 2851–2854.
- (26) Berret, J.-F.; Roux, D. C.; Porte, G. Isotropic-to-Nematic Transition in Wormlike Micelles under Shear. *J. Phys. II* **1994**, *4* (8), 1261–1279.
- (27) Rothstein, J. P. Transient Extensional Rheology of Wormlike Micelle Solutions. *J. Rheol.* **2003**, *47*, 1227–1247.
- (28) López-González, M. R.; Holmes, W. M.; Callaghan, P. T.; Photinos, P. J. Shear Banding Fluctuations and Nematic Order in Wormlike Micelles. *Phys. Rev. Lett.* **2004**, *93*, No. 268302.
- (29) Hu, Y.; Lips, A. Kinetics and Mechanism of Shear Banding in an Entangled Micellar Solution. *J. Rheol.* **2005**, *49*, 1001–1027.
- (30) Miller, E.; Rothstein, J. P. Transient Evolution of Shear-Banding Wormlike Micellar Solutions. *J. Non-Newtonian Fluid Mech.* **2007**, *143*, 22–37.
- (31) Pipe, C.; Kim, N. J.; Vasquez, P.; Cook, L.; McKinley, G. Wormlike Micellar Solutions: II. Comparison between Experimental Data and Scission Model Predictions. *J. Rheol.* **2010**, *54*, 881–913.
- (32) Rothstein, J. P. Strong Flows of Viscoelastic Wormlike Micelle Solutions. *Rheol. Rev.* **2008**, *6*, 1–46.
- (33) Drye, T. J.; Cates, M. E. Living Networks: The Role of Cross-Links in Entangled Surfactant Solutions. *J. Chem. Phys.* **1992**, *96* (2), 1367–1375.
- (34) Kadoma, I. A.; Ylitalo, C.; van Egmond, J. W. Structural Transitions in Wormlike Micelles. *Rheol. Acta* **1997**, *36* (1), 1–12.
- (35) Israelachvili, J. N. *Intermolecular and Surface Forces*; Academic Press: London, 1992.
- (36) Berret, J.-F. *Molecular Gels: Materials with Self-Assembled Fibrillar Networks*; Weiss, R. G.; Terech, P., Ed.; Springer: Netherlands, 2005.
- (37) Gittes, F.; MacKintosh, F. C. Dynamic Shear Modulus of a Semiflexible Polymer Network. *Phys. Rev. E* **1998**, *58*, R1241–R1244.
- (38) Morse, D. C. Viscoelasticity of Concentrated Isotropic Solutions of Semiflexible Polymers. 1. Model and Stress Tensor. *Macromolecules* **1998**, *31*, 7030–7043.
- (39) Tassieri, M.; Ramírez, J.; Karayiannis, N. C.; Sukumaran, S. K.; Masubuchi, Y. i-Rheo GT: Transforming from Time to Frequency Domain without Artifacts. *Macromolecules* **2018**, *51*, 5505–5508.
- (40) Magid, L. J.; Han, Z.; Li, Z.; Butler, P. D. Tuning the Contour Lengths and Persistence Lengths of Cationic Micelles: The Role of Electrostatics and Specific Ion Binding. *J. Phys. Chem. B* **2000**, *104*, 6717–6727.
- (41) Sommer, C.; Pedersen, J. S.; Egelhaaf, S. U.; Cannavacciuolo, L.; Kohlbrecher, J.; Schurtenberger, P. Wormlike Micelles as

“Equilibrium Polyelectrolytes”: Light and Neutron Scattering Experiments. *Langmuir* **2002**, *18*, 2495–2505.

(42) Cannavacciuolo, L.; Pedersen, J. S.; Schurtenberger, P. Monte Carlo Simulation Study of Concentration Effects and Scattering Functions for Polyelectrolyte Wormlike Micelles. *Langmuir* **2002**, *18* (7), 2922–2932.

(43) Schubert, B. A.; Kaler, E. W.; Wagner, N. J. The Microstructure and Rheology of Mixed Cationic/Anionic Wormlike Micelles. *Langmuir* **2003**, *19*, 4079–4089.

(44) Nettesheim, F.; Wagner, N. J. Fast Dynamics of Wormlike Micellar Solutions. *Langmuir* **2007**, *23* (10), 5267–5269.

(45) Porte, G.; Marignan, J.; Bassereau, P.; May, R. Shape Transformations of the Aggregates in Dilute Surfactant Solutions: A Small-Angle Neutron Scattering Study. *J. Phys. (Paris)* **1988**, *49* (3), 511–519.

(46) Cates, M. E.; Candau, S. J. Statics and Dynamics of Worm-like Surfactant Micelles. *J. Phys.: Condens. Matter* **1990**, *2* (33), 6869–6892.

(47) Clark, A. H.; Ross-Murphy, S. B. Structural and Mechanical Properties of Biopolymer Gels. *Adv. Polym. Sci.* **1987**, *83*, 57–192.

(48) Schuldt, C.; Schnauß, J.; Händler, T.; Glaser, M.; Lorenz, J.; Golde, T.; Käs, J.; Smith, D. M. Tuning Synthetic Semiflexible Networks by Bending Stiffness. *Phys. Rev. Lett.* **2016**, *117*, No. 197801.

(49) Tassieri, M. Dynamics of Semiflexible Polymer Solutions in the Tightly Entangled Concentration Regime. *Macromolecules* **2017**, *50*, 5611–5618.